

Stochastic Resonance and Anti-resonance in an Underdamped Josephson Junction

Guozhu Sun, Jian Chen, Weiwei Xu, Zhengming Ji, Lin Kang, Peiheng Wu,
Research Institute of Superconductor Electronics, Department of Electronic Science
and Engineering, Nanjing University, Nanjing, 210093, China,
Guanfeng Mao, Ning Dong, Yang Yu^{*}, and Dingyu Xing
National Laboratory of Solid State Microstructures and Department of Physics,
Nanjing University, Nanjing, 210093, China.

Abstract

Stochastic resonance and anti-resonance were observed in an underdamped real physical system, i.e., a Josephson tunnel junction. With a weak sinusoidal driving force applied, the thermal activated escape from a potential well underwent resonance-like behavior as a function of the driving frequency. The resonance also depended on the initial phase of the periodic driving signal. The average escape time exhibited a minimum (resonance escape) and a maximum (anti-resonance escape) for the initial phase of 0 and π , respectively. Numerical simulations showed good agreement with the experimental results.

PACS: 02.50.-r, 05.40.-a, 74.50.+r

For a heavily damped bistable system, fluctuational forces can cause transitions between two metastable states. If we apply a weak periodic driving force to the system, the hopping rate between the two states will synchronize with the driving frequency, resulting in a statistically resonant phenomenon, i. e., stochastic resonance [1]. Since its first observation in early 1980s [2-5], stochastic resonance has found important applications in nonlinear optics, solid-state devices, chemical reactions and neurophysiology [1]. The notion of stochastic resonance has been extended to different systems such as non-bistable systems [6]. Recently, Yu *et al.* observed resonant phenomena in an underdamped system subjected to a piecewise driving force [7]. Extension of the scope of stochastic resonance to underdamped systems will thus open a new field in the studies of dynamic systems.

In this letter, we investigated the thermal activated escape out of a potential well in an underdamped Josephson tunnel junction. It was found that the escape rates could be enhanced or suppressed by a weak periodic force with different initial phases, indicating that the idea of stochastic resonance could be applied to underdamped non-bistable systems. In addition, to the best of our knowledge, this is the first report of the phase dependence of stochastic resonance. We name the suppression of the escape rate stochastic anti-resonance, which may be applicable to overdamped systems as well.

The equation of motion of a current-biased Josephson tunnel junction is identical to the classical equation of motion of a particle moving in a washboard potential [8]. For the bias current $I_b < I_c$, where I_c is the critical current of the Josephson junction,

the potential has a series of metastable wells with barrier height

$$\Delta U = 2E_J(\sqrt{1-i^2} - i \cos^{-1} i) \quad (1)$$

where $i = I_b / I_c$ is the normalized bias current, $E_J = I_c \Phi_0 / 2 \pi$ is the Josephson coupling energy, and $\Phi_0 = h / 2e$ is the flux quantum. A junction initially trapped in a potential well (corresponding a zero voltage drop on the junction) can be activated out of the well by thermal fluctuation. The lifetime of the zero voltage state is given by [9]

$$\tau \equiv 1/\Gamma_t = \left(a_t \frac{\omega_p}{2\pi} \right)^{-1} \exp(\Delta U / k_B T), \quad (2)$$

with $\omega_p = \omega_{p0}(1-i^2)^{1/4} \equiv \sqrt{2\pi I_c / \Phi_0 C} (1-i^2)^{1/4}$ being the small oscillation frequency of the particle at the bottom of the well, and k_B being the Boltzmann's constant. The prefactor a_t is weakly dependent on the damping of the system and can be treated as a constant $a_t \approx 1$ [10].

The sample used in this study was a NbN/AlN/NbN Josephson tunnel junction. The critical temperature T_c was about 16 K. The $I-V$ characteristic measurements showed that the junction was of high quality with large hysteresis, indicating the system was a highly underdamped system [11]. The sizes of the junction were 6 $\mu\text{m} \times$ 6 μm . The critical current and the capacitance of the junction were $I_c \sim 1.6$ mA and $C \sim 1.8$ pF. The sample was mounted on a chip carrier that was enclosed in a helium-filled oxygen-free copper sample cell, which was then dipped into liquid helium. The junction was magnetically shielded by a Mu-metal cylinder. All electrical leads that connected the junctions to room temperature electronics were carefully filtered by RC filters (with a cutoff frequency of about 1 MHz) and Cu-powder filters

(with a cutoff frequency of about 1 GHz). Battery-powered low-noise preamplifiers were used for all measurements. The experiments were performed in a copper shielded room.

The escape times of the junction were directly measured using the time-domain technique [12]. For each escape event, we started the cycle by ramping up the bias current to a value I_b , which was very close to I_c ($I_b \sim 0.99I_c$), and maintaining at this level for a period of waiting time. A sinusoidal current $I_{ac} = 2i_{ac} \sin(2\pi ft + \varphi_0)$ was added to the bias current during the waiting time, where $t = 0$ when the bias current reached I_b . Usually, i_{ac} was much smaller than I_b . The junction voltage was fed to a timer, which was triggered by the sudden voltage jump when the junction switched from zero-voltage state to finite-voltage state, to record escape time t_{esc} . The bias current I_b was then decreased to zero, returning the junction to the zero-voltage state (Fig.1b) . The process was repeated about 10^4 times to obtain an ensemble of the escape time. The average time of the ensemble represented the mean thermal activation escape time $\langle t_{esc} \rangle$. Then we changed f , and measured another $\langle t_{esc} \rangle$. By plotting $\langle t_{esc} \rangle$ as a function of f we observed the resonant behavior. It was worth to mention the difference between our experiments and those for the other systems [1]. In those measurements, f was fixed and the resonance was observed by tuning the noise level. That was equivalent to changing the temperature while keeping f constant in our experiments. Here we chose f as an adjustable parameter because it can be controlled more precisely in our experiments.

In Fig. 2a, for various bias currents, we showed $\langle t_{esc} \rangle$ as a function of f with the

initial phase $\varphi_0 = 0$. On each curve, a resonant valley could be clearly seen. The resonant frequencies f_{res} were about several kHz, which was 10^5 times smaller than the oscillation frequency ω_p . Therefore we could exclude the dynamic resonance, which required $f \sim \omega_p$ [13]. Moreover, when we increased I_b , the escape rate increased. Consequently, f_{res} increased in order to match the escape rate (Fig. 2b). These were the signatures of stochastic resonance. From the best fit in Fig. 2b, we obtained that the matching condition was

$$4\langle t_{esc} \rangle \simeq 1/f_{res}, \quad (3)$$

which was a factor of two different from that of the bistable systems [1]. Qualitatively, our system was a non-bistable open system. Unlike the double well potential, there was no probability to jump backwards here. Therefore, the escape rate was almost doubled and we got the modified resonant condition (3).

For $\varphi_0 = \pi$, it is very interesting that we observed resonant peaks at the matching condition (Fig. 3a). The junction actually had the longest average escape time at f_{res} thereby we called it stochastic anti-resonance. This indicates that the system was not smart enough to always escape from the potential well with the lowest barrier height. The origin of stochastic resonance is just the synchronization of the escape rate and driving frequency. If the barrier height is a minimum at the matching condition, we observe a valley. If the barrier height is a maximum, on the contrary, we get a peak.

Therefore, we expect that $\langle t_{esc} \rangle$ exhibits no clear resonant behavior if the initial phase changes randomly for each t_{esc} . In Fig. 4, we showed $\langle t_{esc} \rangle$ as a function of the

f with random φ_0 . Neither valley nor peak was observed. The escape time kept decreasing until the frequency satisfied $\langle t_{esc} \rangle \simeq 1/f_{res}$. For $f > f_{res}$, the effect of the periodical driving force was saturated and $\langle t_{esc} \rangle$ displayed almost no change.

While it is quite challenging to analytically solve the equation of motion of the unerdamped system, we did numerical simulations in order to confirm our experimental observations. Shown in Fig. 5 and Fig. 6 are some examples of the simulation results where we can see clearly all the features of the stochastic resonance observed in the experiments. In addition, by numerical simulations, the matching condition for stochastic resonance and anti-resonance was found to be $\langle t_{esc} \rangle \simeq 0.23/f_{res}$, very close to the experimental value.

Our experiments and numerical simulations indicate that stochastic resonance is a ubiquitous phenomenon. It may happen in all dynamic systems, including both overdamped and underdamped systems. Therefore, stochastic anti-resonance, observed in this work in an underdamped system, should be expectable in overdamped systems too. This may be helpful for the applications using overdamped systems [1].

In summary, for the first time we observed stochastic resonance in an underdamped Josephson junction from both experiments and numerical simulations. The matching condition for the non-bistable open system was $4\langle t_{esc} \rangle \simeq 1/f_{res}$ in the experiments and $4\langle t_{esc} \rangle \simeq 0.92/f_{res}$ in the simulations. In addition, stochastic resonance is sensitive to the initial phase of the periodic force, and displayed anti-resonance for an initial phase of π . This confirms that stochastic resonance is an

average effect and different from dynamic resonance. We believe that stochastic resonance is a ubiquitous phenomenon and the stochastic anti-resonance can be observed also in overdamped dynamic systems.

This work is partially support by the National Natural Science Foundation of China (10474036) , the National Basic Research Program of China, 973 Program (2006CB61006) and the Doctoral Funds of Ministry of Education of the People's Republic of China (2004028033).

Figure Captions

Fig. 1. (a) Washboard potential and equivalent circuit (inset) of a current biased Josephson tunnel junctions with $I_b < I_c$. (b) Schematic time profile for measuring the escape time of a Josephson junction subjected to a weak sinusoidal force.

Fig. 2. (a) Average escape time as a function of the driving frequency at 4.2 K for various normalized bias currents which are marked below the curves. The initial phase was $\varphi_0 = 0$, and $i_{ac} \sim 0.002 I_b$. The valleys indicate stochastic resonance, with the resonant frequency depending on the bias current remarkably. (b) The minimum average escape time vs. inverted resonant frequency. The dashed line is the best fit with a slope of 0.26 ± 0.03 .

Fig. 3. (a) Average escape time as a function of the driving frequency for different bias currents (marked on the curves) with the initial phase $\varphi_0 = \pi$. The temperature was 4.2 K and $i_{ac} \sim 0.002 I_b$. Resonant peaks, instead of valleys, were clearly observed. (b) The maximum average escape time vs. inverted resonant frequency. The dashed line is the best fit with slope 0.23 ± 0.01 .

Fig. 4. Average escape time $\langle t_{esc} \rangle$ as a function of the driving frequency for different bias currents at 4.2 K. For each t_{esc} , the initial phase φ_0 was randomly selected. Statistically, there was neither valley nor peak on each curve.

Fig. 5. The numerically calculated average escape time vs. the frequency of the sinusoidal driving force with $\varphi_0 = 0$. The parameters used in the simulations were: $T = 4.2$ K, $C = 1.8$ pF, $R = 2$ ohm, $I_c = 1.6$ mA, $i_{ac} \sim 0.002 I_c$. The minimum of the average escape time moved to the higher frequency when the bias current increased,

consistent with the experimental observations. The matching condition obtained from the calculation was $\langle t_{esc} \rangle \approx 0.23/f_{res}$, showing quantitative agreement with the experiment observations.

Fig. 6. The numerically calculated average escape time vs. the frequency of the sinusoidal driving force with various initial phase conditions $\varphi_0 = 0$ (square), $\varphi_0 = \pi$ (open circle), and $\varphi_0 = \text{random number}$ (triangle). $I_b = 0.995I_c$, and other parameters were the same as those used in Fig. 5.

References

*yuyang@nju.edu.cn

1. L. Gamaitoni, P. Hänggi, P. Jung, and F. Marchesoni, Rev. Mod. Phys. **70**, 223 (1998)
2. Benzi, R., G. Parisi, A. Sutera, and A. Vulpiani, 1982, Tellus **34**, 10.
3. Benzi, R., A. Sutera, G. Parisi, and A. Vulpiani, 1983, SIAM (Soc. Ind. Appl. Math.) J. Appl. Math. **43**, 565.
4. Benzi, R., A. Sutera, and A. Vulpiani, 1981, J. Phys. A **14**, L453.
5. Fauve, S., and F. Heslot, 1983, Phys. Lett. **97A**, 5.
6. Longtin, A., 1993, J. Stat. Phys. **70**, 309
7. Y. Yu and S. Han, Phys. Rev. Lett. **91**, 127003 (2003).
8. W. C. Stewart, Appl. Phys. Lett. **12**, 277 (1968); D. E. McCumber, J. Appl. Phys. **39**, 3133 (1968).
9. T. A. Fulton, L. N. Dunkleberger, Phys. Rev. B **9**, 4760 (1974).
10. P. Hänggi, P. Talkner, and M. Borkovec, Rev. Mod. Phys. **62**, 251 (1990).
11. A. Barone and G. Paterno, *Physics and Applications of the Josephson Effect* (John Wiley and Sons, New York, 1982).
12. S. Han *et al.* Science **293**, 1457 (2001); Y. Yu *et al.*, Supercond. Sci. Technol. **15**, 555 (2002).
13. M. H. Devoret, J. M. Martinis, D. Esteve, and J. Clarke, Phys. Rev. Lett. **53**, 1260 (1984)

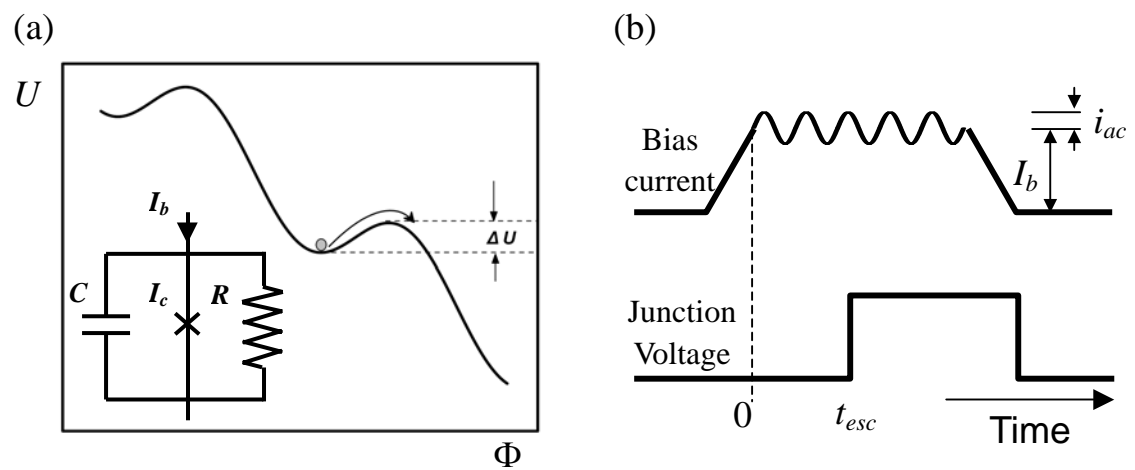


Fig. 1 G. Sun *et al.*

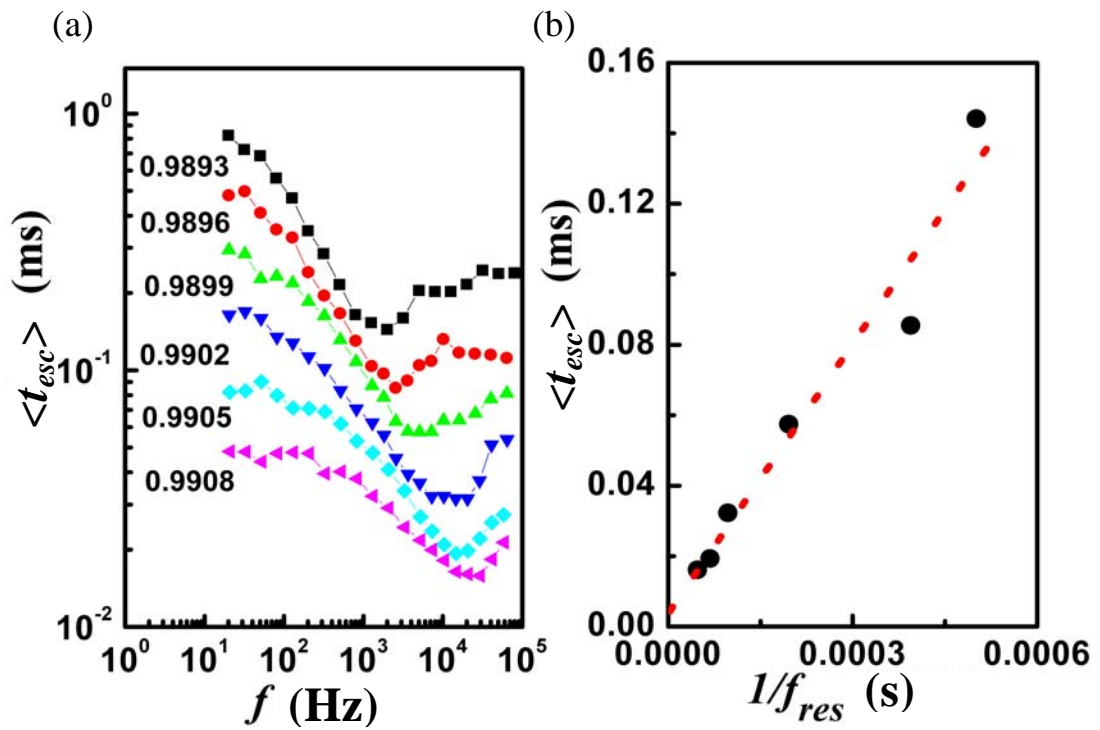


Fig. 2 G. Sun *et al.*

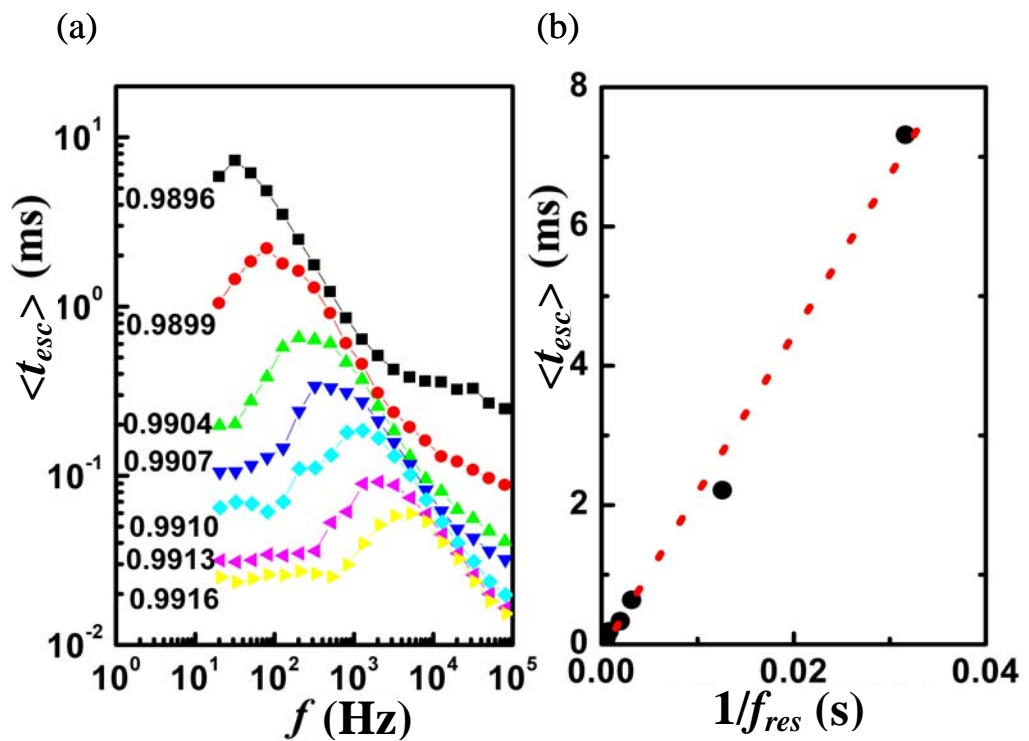


Fig. 3 G. Sun *et al.*

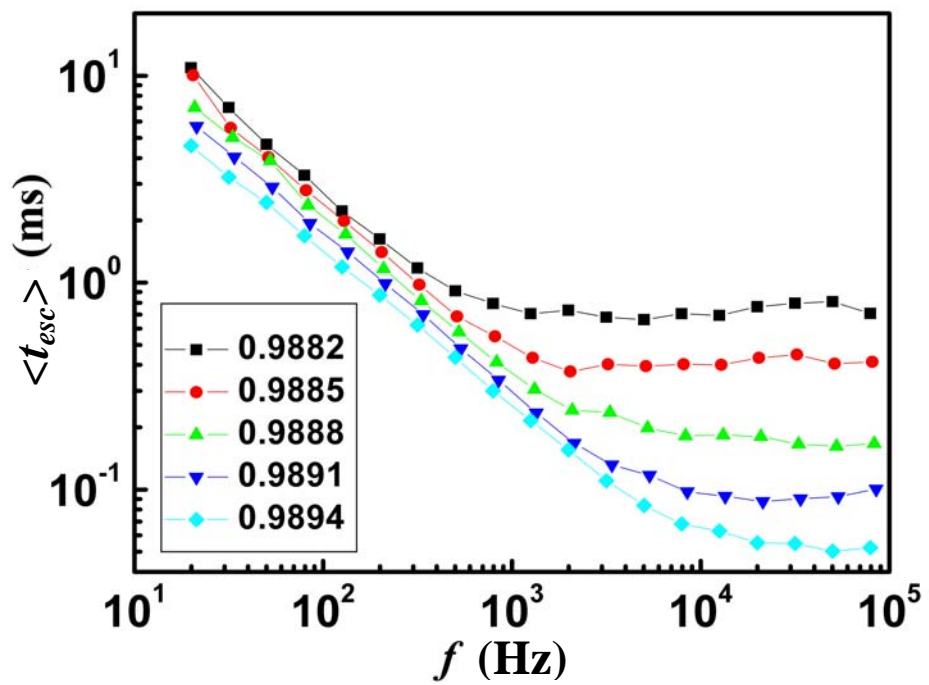


Fig. 4 G. Sun *et al.*

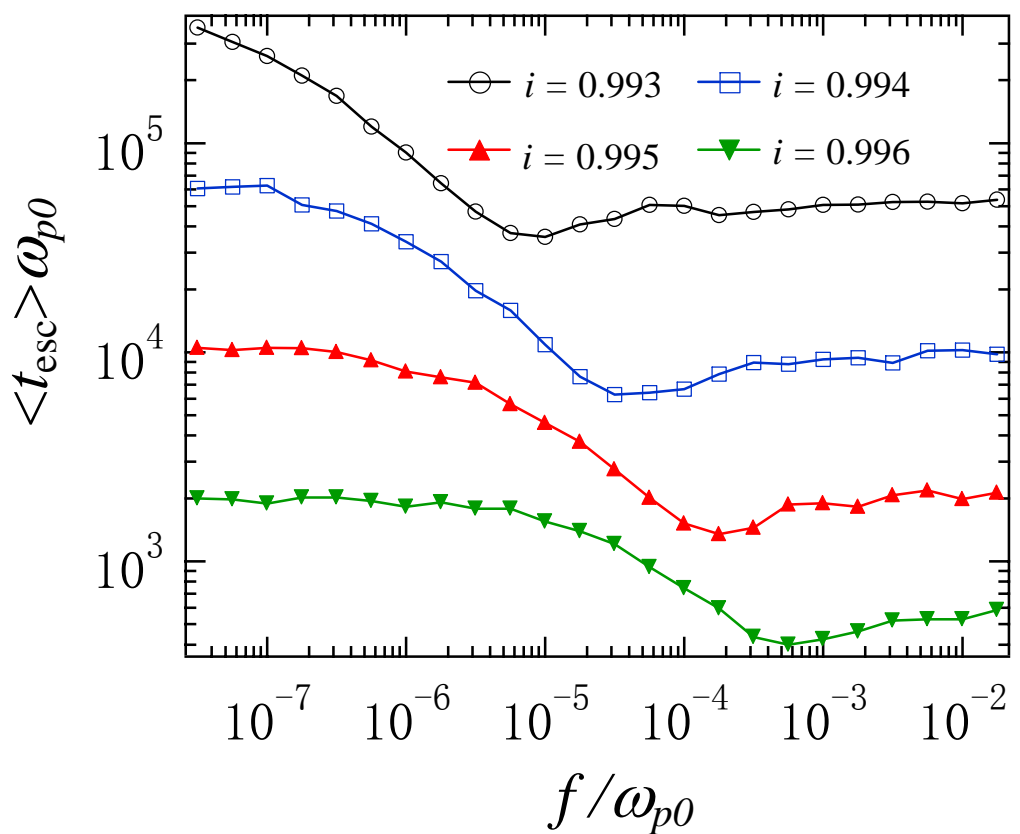


Fig. 5 G. Sun *et al.*

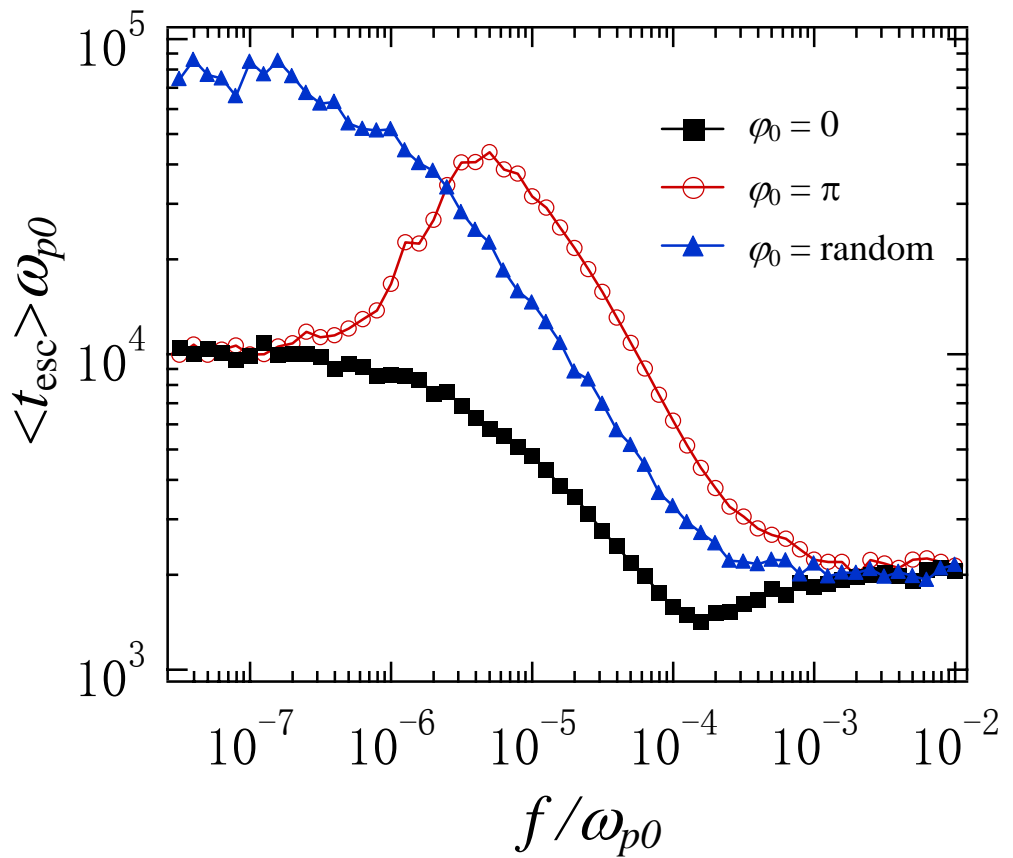


Fig. 6 G. Sun *et al.*